Physics and Imaging in Radiation Oncology 3 (2017) 5–10

Contents lists available at ScienceDirect

Physics and Imaging in Radiation Oncology

journal homepage: www.elsevier.com/locate/phro

Impact of lung density on the lung dose estimation for radiotherapy of breast cancer

Emma Hedin, Anna Bäck, Roumiana Chakarova *

Dept of Radiation Physics, Inst of Clinical Sciences, Sahlgrenska Academy, University of Gothenburg, Gothenburg, Sweden
Dept of Medical Physics and Biomedical Engineering, Sahlgrenska University Hospital, Gothenburg, Sweden

ARTICLE INFO

Article history:
Received 25 January 2017
Received in revised form 3 June 2017
Accepted 3 July 2017

Keywords:
Breast cancer
Lung dose
DIBH
Acuros XB
Monte Carlo

ABSTRACT

Background and purpose: To investigate the impact of the clinical implementation of a deterministic particle transport method on the lung dose evaluation for radiotherapy of breast cancer focusing on dosimetric effects of the lung density.

Material and methods: Fourteen patients with left sided breast cancer having both deep inspiration breath hold (DIBH) and free breathing CT scans were studied. Lung density variations for 157 patients treated under DIBH were quantified and the cases with the lowest lung densities for breast and for loco regional treatment added to the study. Dose calculations were performed with the class-b type algorithm AAA and the deterministic algorithm Acuros XB. Monte Carlo method was utilized as reference. Differences in the dose distributions were evaluated by comparing DVH parameters.

Results: Lung density variations between 0.08 and 0.3 g/cm^3 and between 0.02 and 0.25 g/cm^3 were found for loco-regional and tangential breast treatments under DIBH, respectively. Lung DVH parameters for patients with medium and high lung density obtained by the different algorithms agreed within 3%. Larger differences were observed for low lung density cases where the correction based algorithm underestimated V_{10Gy} and overestimated V_{40Gy} by up to 5%. The least affected parameter, V_{20Gy}, deviated by less than 2% for all cases and densities.

Conclusions: Dosimetric constrains for lung based on V_{20Gy} required minimum changes due to implementation of the new algorithm regardless of breathing technique or type of treatment. Evaluation criteria utilizing V_{10Gy} or V_{40Gy} needed reconsideration, especially for treatments under DIBH involving low lung density.

1. Introduction

Radiotherapy of breast cancer involves complex anatomy and regions of highly different densities; soft tissue, lung and bone, surrounding air. The lung density may substantially decrease when utilizing respiratory gating technique such as deep inspiration breath hold (DIBH) in order to limit the radiation dose to the heart. An accurate determination of the dose distribution in lung requires advanced dose calculation algorithms. Type-a algorithms, using inhomogeneity corrections along the ray direction only, have been gradually replaced by type-b algorithms capable to approximate the lateral electron transport. Both use dose kernels calculated in water and handle different tissues by density based corrections.

More advanced methods explicitly model the interaction of radiation with matter solving the Linear Boltzmann Transport Equation (LBTE). Monte Carlo (MC) is well established stochastic method indirectly obtaining the LBTE solution. Because of the relatively long computational time and the statistical noise of the result, it is mostly used as a reference method when evaluating dose distributions from the treatment planning systems. An alternative approach has been recently applied to address medical physics problems utilizing a deterministic method for numerical solution of the LBTE [1]. The accuracy of the new algorithm has been fundamentally investigated [1–6] and found to be comparable to MC.

Important step toward the clinical implementation of the new method is to ensure the validity of the old treatment planning criteria or to reconsider them. Dosimetric predictors of radiation induced lung complications involved in the plan evaluation are currently related to dose distributions produced by correction

* Corresponding author at: Department of Radiation Physics, Gula straket 2B, Sahlgrenska University Hospital, SE-413 45 Gothenburg, Sweden.
E-mail address: roumiana.chakarvoa@vgregion.se (R. Chakarova).

http://dx.doi.org/10.1016/j.phro.2017.07.001

based algorithms. The impact of the algorithm change on the dose parameters needs to be investigated in order to take advantage of previous clinical experience. Whether type-b algorithms over- or underestimate dose was shown to depend on field size, beam energy and electron density [3,7,8]. Thus, results from comparative dosimetric studies for diverse radiation treatments cannot be automatically translated to dose distributions in lung tissue for breast cancer treatment.

Studies for breast cancer treatments confirmed the impact of the lung density on the accuracy of the dose determination [7,9]. Deviations between lung dose distributions determined by the explicit and correction based algorithms were larger in cases of DIBH compared to FB for tangential 6 MV beams [9]. Dosimetric differences for commonly used field in field techniques utilizing different beam energies as well as for treatment techniques of more advanced breast cancer including lymph nodes were not examined.

In this work a comparative dosimetric study was performed of the impact of the clinical implementation of the deterministic radiation transport algorithm on the lung dose estimation for tangential as well as loco-regional treatment of breast cancer. The effect of the lung density on the dose determination was investigated by considering clinical plans for FB as well as DIBH. The lung density in DIBH CT scans for a large population was evaluated in order to quantify the variations. The cases with lowest lung density were identified and the corresponding dose distributions studied in detail with MC method as a reference.

2. Method and materials

2.1. Clinical material

Fourteen patients with left sided breast cancer having both DIBH and FB CT scans were included in the dosimetric study. The scans were acquired with 3 mm slice separation on a Toshiba Aquillion LB CT-scanner (Toshiba Medical Systems). The double scans were motivated clinically by the newly installed breathing adaptation system, the Varian real-time position management system (RPM, Varian Medical Systems). The FB CT scan were supposed to enable treatment without adaptive breathing in case of system failure. Five out of fourteen patients underwent loco-regional (LGL) treatment with tangential fields covering the breast tissue and anterior-posterior fields covering supraclavicular lymph nodes. Rest of the patients underwent radiotherapy of breast cancer by tangential fields covering the breast tissue.

The tumor was delineated by physicians and lung tissue was automatically defined by the clinical segmentation wizard in Eclipse treatment planning system. The prescribed dose was 50 Gy at 2 Gy per fraction with at least 95% isodose covering the PTV. The treatments were planned with 6 MV and 15 MV photon beams delivered by Varian accelerator with a static multileaf collimator (MLC). Two treatment plans, one on the FB CT scan and one on the DIBH CT scan, were prepared for each patient.

The lung tissue densities were evaluated for the fourteen patients with double CT scans as well as for a large population of 157 breast cancer patients treated with DIBH technique during one year. The two cases of lowest lung density identified in the large population, one for LGL treatment and one for breast treatment, were added to the dosimetric study.

2.2. Evaluation of lung density variations

The lung density was determined for each CT scan as the average lung density in a two dimensional rectangular region of interest (ROI) in a transversal plane. The ROI was placed within the 15% isodose line and the size was at least 20 × 20 pixels (1 mm resolution). The ROI was placed in the isocenter plane of both the LGL and breast treatment plans. For the LGL cases the isocenter plane was located at the junction between the tangential fields (covering

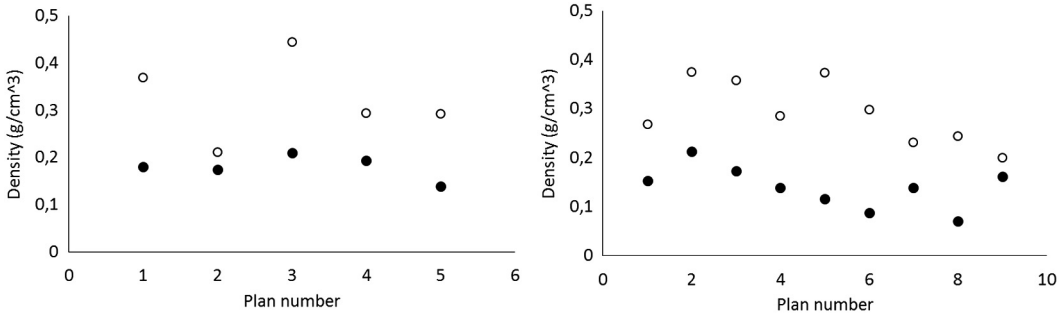

Fig. 1. The lung density in the isocenter plane for the patients given LGL (left) and tangential breast (right) treatments with plans for FB (open circles) and DIBH (filled circles).

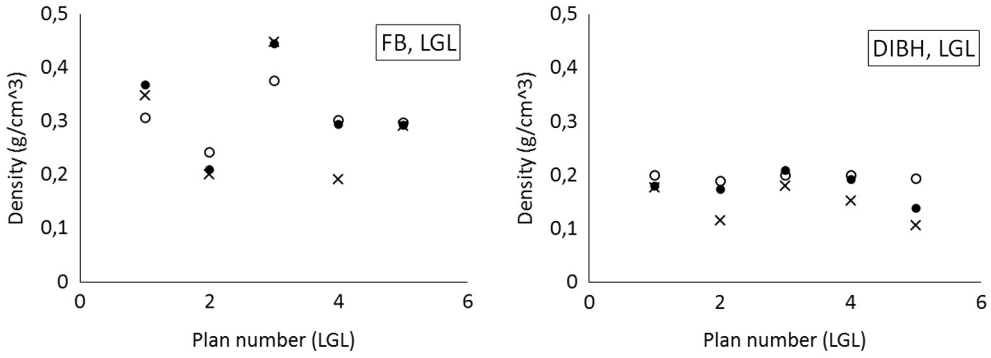

Fig. 2. The lung density for the 5 LGL cases, FB (left) DIBH (right), measured at three different planes: isocenter (filled circles); caudal plane across tangential fields (crosses); cranial plane across anterior/posterior field (open circles).

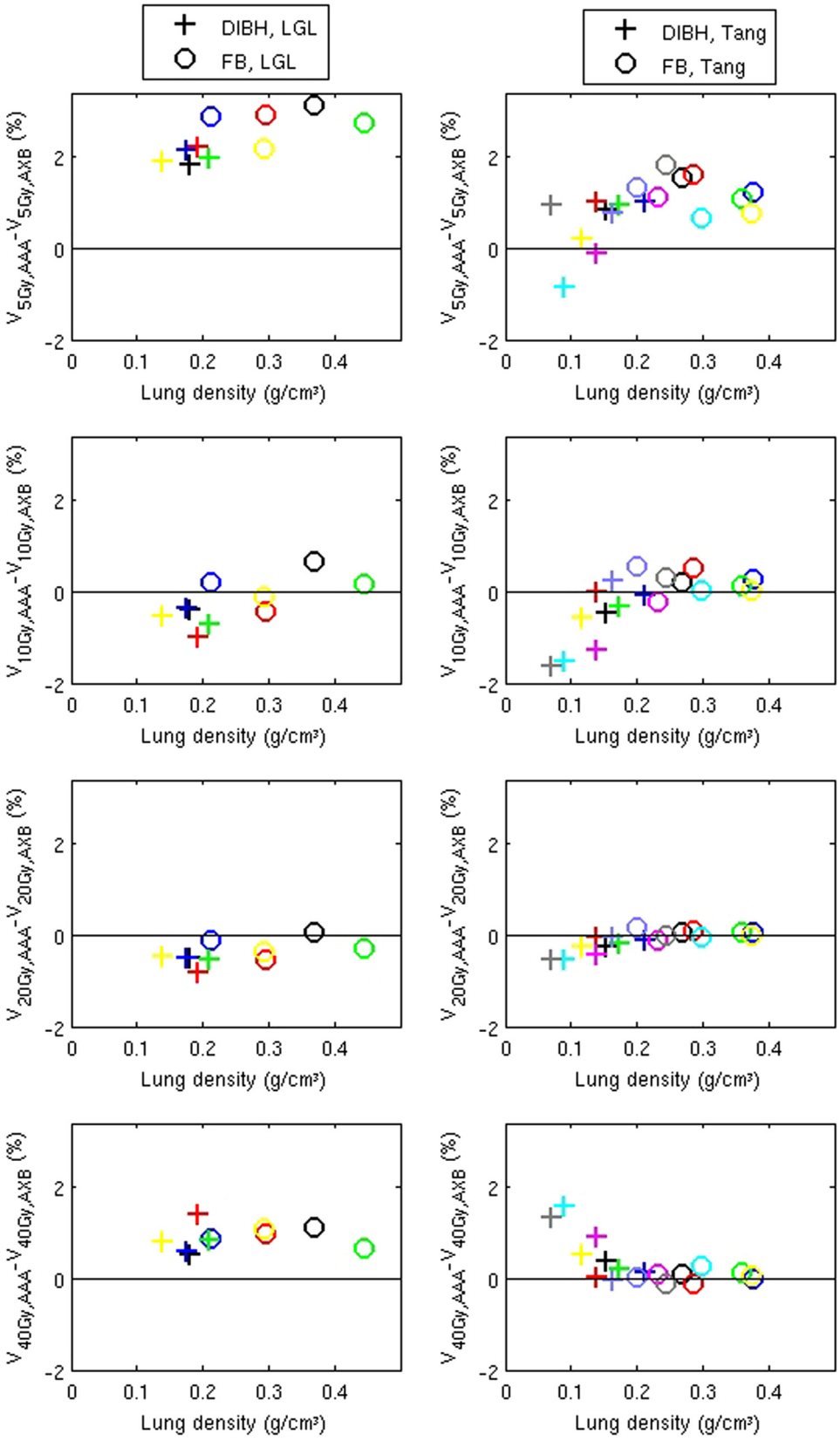

Fig. 3. Difference between V_{5Gy}, V_{10Gy}, V_{20Gy} and V_{40Gy} for ipsilateral lung calculated with AAA and AXB. Left: 5 FB (O) and 5 DIBH (+) loco-regional treatment plans. Right: 9 FB (O) and 9 DIBH (+) tangential (right) breast treatment plans. Each patient has a specific color indicating which O and + that belongs to that patient (each patient has two CT scans – one FB and one DIBH). Lung density in isocenter plane on the x-axis.

the breast tissue) and the anterior-posterior fields (covering the clavicular fossa), i.e. approximately 5 cm below the top of the lung in the craniocaudal direction. For the breast cases the isocenter plane was approximately in the middle of the craniocaudal opening of the tangential fields.

The lung density was measured in two additional planes for the five LGL-cases with both FB and DIBH CT scans. Those planes were i) centrally in the tangential field, i.e. a measurement plane equivalent to the plane used for the breast treatment cases and ii) in a plane between the isocenter at the cranial tip of the lung, i.e. a measurement plane in the cranial part of the lung.

2.3. Calculation algorithms

The treatment plans were designed in the Eclipse treatment planning system by the correction based algorithm AAA version 13.6.23, currently in use in our hospital. They have been recalculated by the deterministic algorithm explicitly solving the LBTE, Acuros XB (AXB) version 13.6.23, using the same number of monitor units, MLC and collimator positions, dynamic wedges and beam arrangement. The two cases from the large population with the lowest lung density were planned by AAA and recalculated by AXB as well as by the MC method.

The AAA implementation in the treatment planning system was based on the assumption that all the tissues were composed of water with a density according to the information in the CT scan and electron-density CT calibration curve. For AXB, tissue segmentation was required which involved a mass-density CT calibration curve and a clinical tissue type table with six tissues, i.e. air, lung, adipose tissue, skeletal muscle, cartilage and bone. The density intervals specifying the tissue types were overlapping, i.e. the border between for instance lung/adipose tissues was not sharp but in a given mass density interval both lung and adipose tissue were present. There is no consensus in the clinical praxis regarding dose determination in terms of dose-to-medium or dose-to-water. AXB implementation allowed users choice of reporting dose to water or dose to media. In this study the 'dose-to-water' reporting mode was used for comparison with AAA and the 'dose-to-media' reporting mode was used for comparison with the MC calculations. For both dose reporting modes the AXB fluence calculation was identical and performed in the different tissue types as determined from the CT scan. For dose-to-water calculations, the conversion to dose was made by utilizing the response function for water for each voxel regardless of voxel material determined from the CT scan [10].

The MC method was independent from the treatment planning system and was used as a third method to compare the dosimetric performance of AAA and AXB in the extreme cases selected. The accelerator model, designed within the EGSnrc code package, was developed earlier and validated by the same experimental data used for configuration of AAA and AXB [11–13]. Tissue segmentation was performed by 9 material table with a more detailed presentation of bone tissue types [14,15]. A distinct border between different tissue types was used. To match the AXB calculations with MC as well as possible for air, lung, adipose and muscle, this border was chosen to be the mean of the mass density interval used for mixed materials in AXB. The necessary number of histories per area unit in the MC calculations was evaluated by a test calculation for one of the treatment fields in the particular plan. The number of histories in the test calculation was increased until the dose-volume histograms (DVHs) for one field calculated with different number of histories converged according to visual exam.

A clinically realistic dose grid of 2 mm in the transverse plane and 3 mm between CT-slices was used for all dose calculations (including MC). The dose calculation methods were compared for all treatment plans by analysis of ipsilateral lung DVH parameters V_{5Gy}, V_{10Gy}, V_{20Gy} and V_{40Gy}, where V_{XGy} denotes the lung volume receiving X Gy. Differences in the values were expressed in percentage points.

3. Results

The lung densities at the isocenter plane for FB scans were consistently higher compared to the corresponding ones under DIBH for each of the fourteen patients with double CT scans (Fig. 1). The same tendency was observed for the lung densities at the two additional planes analyzed for the five out of fourteen patients receiving LGL treatment (Fig. 2). Thus, all the three lung regions studied were affected by the deep inspiration. For the FB CT-scans the densities of the different planes were not ordered, (Fig. 2 left), while for the DIBH CT-scans consistently lower density was obtained at the plane centrally in the tangential field (Fig. 2 right). The deviations between the DVH parameters V_{5Gy}, V_{10Gy}, V_{20Gy} and V_{40Gy}, for the ipsilateral lung obtained by the two clinical algorithms were within 3.1% for each of the fourteen patients (Fig. 3). The smallest differences were seen for the parameter

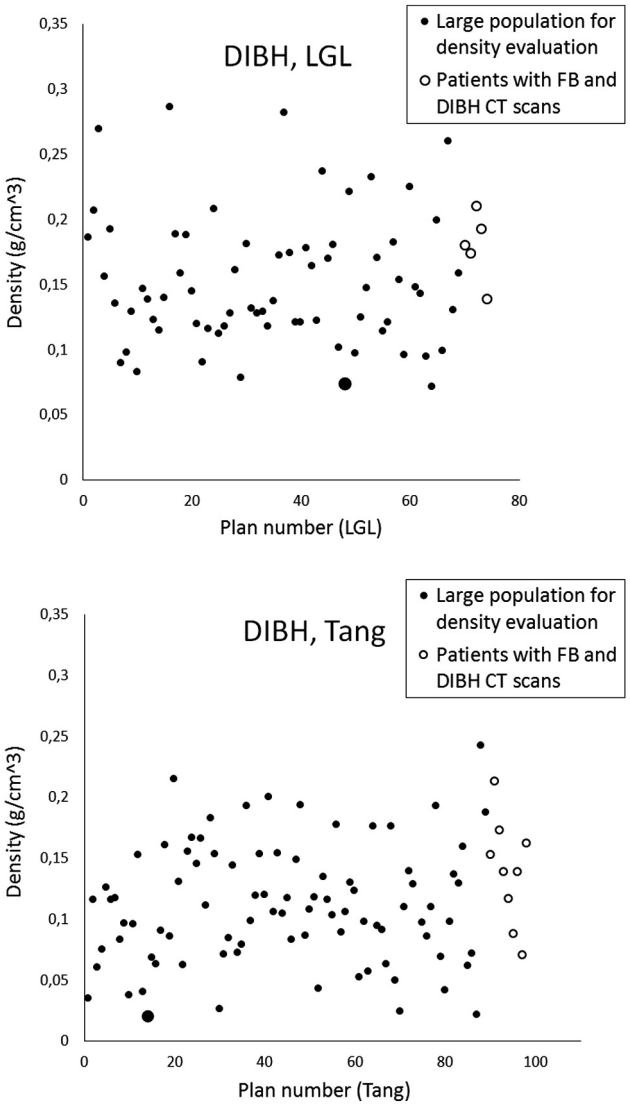

Fig. 4. Lung density in isocenter plane within the 15% isodose for patients planned for LGL (left) and tangential breast (right) treatments that have treatment plans planned on DIBH CT scans. The DIBH CT scan lung density for the patients with both FB and DIBH scans are also shown for comparison. The larger dots indicate the plans chosen for AAA, AXB and MC comparisons.

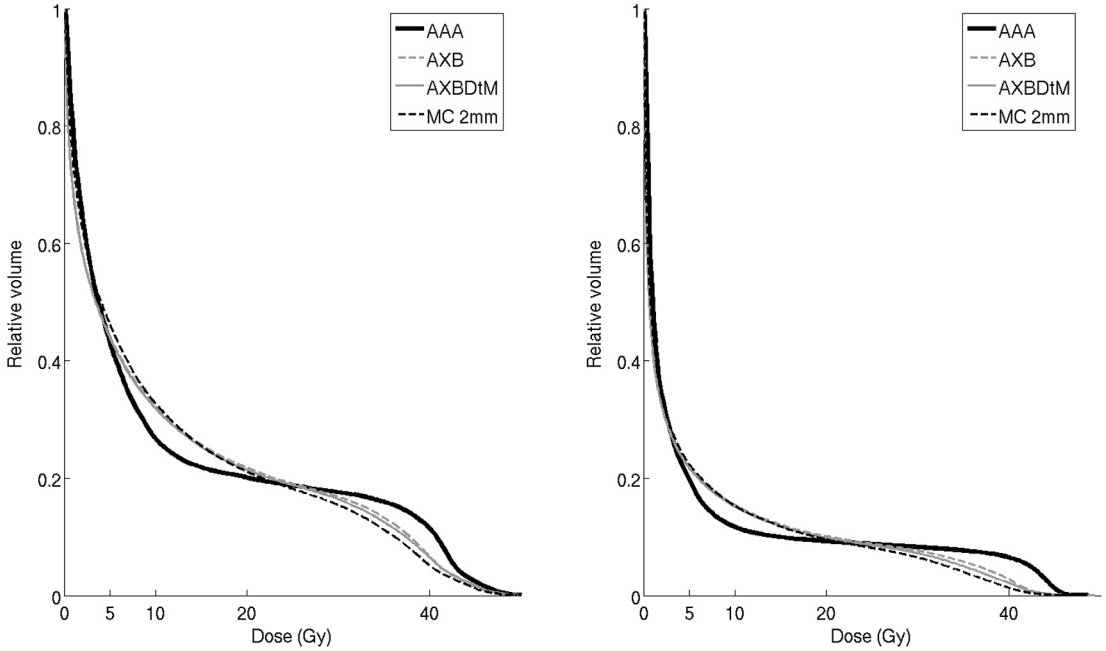

Fig. 5. DVH for ipsilateral lung for a LGL (left) and a tangential (right) breast cancer treatment plan that were planned on the DIBH CT scan with the lowest lung densities observed. Dose calculated with AAA, AXB (dose to water), AXBDtM (dose to medium) and MC (2 mm and 7 mm voxels).

V_{20Gy}; less than 1% for all plans regardless of breathing technique or type of treatment.

Larger variation of the lung densities was obtained for the 157 patients with DIBH CT scans than the corresponding ones for the patients with double CT scans. Lung densities at isocenter plane varied between 0.08 and 0.3 g/cm^3 for LGL treatment and between 0.02 and 0.25 g/cm^3 for tangential breast treatment (Fig. 4). The cases with the lowest lung densities identified in the large population, (Fig. 4), were further evaluated by the clinical dose calculation algorithms as well as by the MC method. The figure illustrates how common the very low density lung tissue is for the DIBH CT scans. The estimation of the mean lung densities based on a small group patients might be misleading. For example, the lung densities of the five patients with double scans receiving LGL treatment were not representative for the large population (Fig. 4).

The dose distributions calculated by the two methods solving the LBTE, AXB and MC, were similar for the two DIBH CT-scans with lowest lung density (Fig. 5). For the LGL treatment, the deterministic method calculated a 3% lower value of V_{5Gy} compared to MC and the rest of the DVH parameters differed by less than 1%. For the breast treatment the difference between the methods for all the DVH parameters considered was less than 1%. The DVH obtained by AAA deviated in both the breast and LGL cases (Fig. 5). The algorithm underestimated the DVH parameters in the low dose region. For the LGL case, the AAA values for V_{5Gy} and V_{10Gy} were lower by 1% and 5%, respectively, compared to AXB. The corresponding values for the breast treatment case were 2% and 4% lower than AXB. The deviation in the high dose DVH region had an opposite sign. AAA was overestimating V_{40Gy} by 5% and 4% for the LGL and breast treatment case, respectively. The smallest deviations were seen for the V_{20Gy} parameter; 2% and 1% for the two treatment cases.

4. Discussion

Decreased lung density in the DIBH CT scan synchronized with larger differences in the DVH parameters V_{10Gy}, V_{20Gy} and V_{40Gy} estimated by the exact and the correction based algorithms for the breast treatment plans (Fig. 3, right column of diagrams). This result was in line with the results from [9] although here plans with mixed 6 and 15 MV beams and field in field technique were used. For the LGL cases investigated the same trend was not visible. This may be due to the different beam arrangement. Furthermore, the LGL treatments were associated with a smaller range of lung densities as compared to the breast treatment (Fig. 4).

In general, the lung densities in the DIBH CT scans for the patient group with both FB and DIBH CT scans included in this study (breast and LGL plans) were distributed between medium to high density according to the density evaluation of the larger population (157 plans) and they did not cover the lowest lung densities. For those medium to high lung density cases, the effect of explicitly modelling the secondary electron transport and tissue heterogeneity was limited but detectable. The effect was more pronounced for the two cases identified with the lowest lung density, (0.08 g/cm^3 and 0.02 g/cm^3 for LGL and tangential treatment, respectively), were deviations up to 5% were obtained in the DVH parameters. It should be noted that different lung densities, for example 0.1 g/cm^3 or 0.15 g/cm^3 can be regarded as low in the literature [2,9]. The evaluation results (Fig. 4) suggest choice of low density between 0.05 and 0.1 g/cm^3.

The DVH parameter least affected by the choice of the dose calculation algorithm was V_{20Gy}. Even in the cases of lowest lung density, the variation of the estimations was below 2%. Thus treatment planning criteria related to this parameter may not need an update during transition to more advance algorithms. This is particularly interesting since V_{20Gy} is a common parameter for estimation of radiation induced lung complications [16]. In general, the differences in the dose distributions are related to the approximations made in the lateral electron transport when the density is very different from water. In the low density lung tissue, the dose from scattered electrons is deposited further away from the interaction point than the correction algorithm predicts. As result, the dose is overestimated in the high dose region (in-field) and underestimated in the low dose region of the lung (outside the radiation field). For the dose prescription used in this work 20 Gy was close to the 50% isodose and therefore the DVH curves for the algorithms of interest intersected close to V_{20Gy}.

The shape differences of the DVH obtained by the type-b and the explicit algorithms for the two cases with the lowest lung density (Fig. 5), resembled differences in lung DVH for breast cancer treatment between type-a and type-b algorithms [17–19]. As a consequence of taking the lateral electron transport into account, the lung volumes receiving low dose increased and these receiving high dose decreased compared to lung dose determination not taking into account the lateral electron transport [18,19]. Type-b algorithm was considered to give results comparable to Monte Carlo data [20]. Typical analysis from the literature, however, referred to breast cancer treatments under FB, i.e. for normal (high lung density). When DIBH technique was utilized and the lung density is low, the approximations in the lateral electron transport in the type-b algorithms are insufficient to achieve good accuracy of the dose determination. The DVHs deviated considerably from these for the more accurate algorithms explicitly simulating the electron transport (Fig. 5).

The utilization of a certain dose calculation algorithm affected the estimation of the dose-response in terms of Normal Tissue Complication Probability (NTCP) for lung due to radiation treatment of breast cancer [18,19]. Published NTCP model parameters based on type-a dose calculation algorithms needed to be corrected in order to make them valid for dose distributions determined by more advanced algorithms [19]. The large differences in the lung dose distributions, obtained here in the low lung density cases, imply that similar corrections of the model parameters would be needed for more accurate prediction of lung toxicity for this group patients treated under DIBH.

Both methods solving LTBE estimated a non-flat DVH with difference less than 1% for all parameters except V_{5Gy}. This parameter was in the steep part of the DVH where a small variation in dose generated a large variation in volume. The statistical noise in the MC calculations was reduced until there was no effect on the DVH therefore the comparison between AXB and MC was reliable. Although the accuracy of the radiation transport simulations was comparable for the two methods, the description of the source was different. The MC simulations included the transport of the radiation through the accelerator head before entering the patient geometry, whereas AXB used analytical sources fitting the accelerator output. The procedures of segmentation and voxelization of patient geometry were not unified. Also, a smaller value of energy level (ECUT) was applied in the MC method. For the DIBH cases investigated, part of the low density lung was interpreted as air. For such low densities the electrons are scattered even further than in ordinary lung. Therefore, differences in the simulation of the electrons were potentially causing differences in dose between the deterministic and the stochastic method. Nevertheless, looking at the dosimetric comparison this effect seemed to be very limited. Thus the two methods were completely independent producing similar lung dose calculation results.

In summary, lung density variations between 0.02 and 0.3 g/cm^3 were estimated for patients treated during DIBH. Lung densities below 0.1 g/cm^3 (for LGL) and below 0.05 g/cm^3 (for tangential breast treatment) were not exceptional. The DVH parameters obtained by the different algorithms agreed within 3% for medium and high lung density and within 5% for low lung density. The least affected parameter was $V_{20Gy,}$ for which the deviations were less than 2% for all cases; for FB or DIBH, for LGL or tangential breast treatment and for all the densities studied. Thus, to minimize changes in the treatment planning criteria due to implementation of more advanced algorithm, V_{20Gy} was a suitable parameter for controlling lung dose. V_{10Gy} was less suitable, because for this parameter the algorithm change would result in a more conservative treatment plan regarding lung dose.

Conflict of interest

None.

Acknowledgement

We would like to acknowledge Elisabeth Wurzinger who has been responsible for treatment planning of two treatment plans per patient for the patients having undergone both DIBH and FB CT-scans.

This study was supported by grants from the King Gustav V Jubilee Clinic Cancer Research Foundation and Lions Cancer Research Foundation of Western Sweden.

References

[1] Vassiliev ON, Wareing TA, McGhee J, Failla G, Salehpour MR, Mourtada F. Validation of a new grid-based Boltzmann equation solver for dose calculation in radiotherapy with photon beams. Phys Med Biol 2010;55:581–98.
[2] Bush K, Gagne IM, Zavgorodni S, Ansbacher W, Beckham W. Dosimetric validation of Acuros XB with Monte Carlo methods for photon dose calculations. Med Phys 2011;38:2208–21.
[3] Fogliata A, Nicolini G, Clivio A, Vanetti E, Cozzi L. Dosimetric evaluation of Acuros XB Advanced Dose Calculation algorithm in heterogeneous media. Radiat Oncol 2011;6:1–15.
[4] Hoffmann L, Jorgensen MB, Muren LP, Petersen JB. Clinical validation of the Acuros XB photon dose calculation algorithm, a grid-based Boltzmann equation solver. Acta Oncol 2012;51:376–85.
[5] Misslbeck M, Kneschaurek P. Comparison between Acuros XB and Brainlab Monte Carlo algorithms for photon dose calculation. Strahlenther Onkol 2012;188:599–605.
[6] Rana S, Rogers K. Dosimetric evaluation of Acuros XB dose calculation algorithm with measurements in predicting doses beyond different air gap thickness for smaller and larger field sizes. J Med Phys 2013;38:9–14.
[7] Fogliata A, Nicolini G, Vanetti E, Clivio A, Winkler P, Cozzi L. The impact of photon dose calculation algorithms on expected dose distributions in lungs under different respiratory phases. Phys Med Biol 2008;53:2375–90.
[8] Kroon PS, Hol S, Essers M. Dosimetric accuracy and clinical quality of Acuros XB and AAA dose calculation algorithm for stereotactic and conventional lung volumetric modulated arc therapy plans. Radiat Oncol 2013;8:1–8.
[9] Fogliata A, Nicolini G, Clivio A, Vanetti E, Cozzi L. On the dosimetric impact of inhomogeneity management in the Acuros XB algorithm for breast treatment. Radiat Oncol 2011;6:1–11.
[10] Failla TW G, Archambault Y, Thompson S. Acuros XB advanced dose calculation for the Eclipse treatment planning system. Varian Medical Systems Clinical perspectives, https://www.varian.com/sites/default/files/resource_attachments/AcurosXBClinicalPerspectives_0.pdf [accessed 17.06.03].
[11] Hedin E, Bäck A, Swanpalmer J, Chakarova R. Monte Carlo simulation of linear accelerator Varian Clinac iX. 2010 Report ID MFT – RADFYS 2010:01, University of Gothenburg.
[12] Chakarova R, Müntzing K, Krantz M, Hedin E, Hertzman S. Monte Carlo optimization of total body irradiation in a phantom and patient geometry. Phys Med Biol 2013;58:2461–9.
[13] Hedin E, Back A, Chakarova R. Jaw position uncertainty and adjacent fields in breast cancer radiotherapy. J Appl Clin Med Phys 2015;16:240–51.
[14] Schneider W, Bortfeld T, Schlegel W. Correlation between CT numbers and tissue parameters needed for Monte Carlo simulations of clinical dose distributions. Phys Med Biol 2000;45:459–78.
[15] Ottosson RO, Behrens CF. CTC-ask: a new algorithm for conversion of CT numbers to tissue parameters for Monte Carlo dose calculations applying DICOM RS knowledge. Phys Med Biol 2011;56:N263–74.
[16] Marks LB, Bentzen SM, Deasy JO, et al. Radiation dose-volume effects in the lung. Int J Radiat Oncol Biol Phys 2010;76(3 Suppl.):S70–6.
[17] Knöös T, Wieslander E, Cozzi L, Brink C, Fogliata A, Albers D, et al. Comparison of dose calculation algorithms for treatment planning in external photon beam therapy for clinical situations. Phys Med Biol 2006;51:5785–8.
[18] Bufacchi A, Nardiello B, Capparella R, Begnozzi L. Clinical implications in the use of the PBC algorithm versus the AAA by comparison of different NTCP models/parameters. Radiat Onc 2013;8:1–13.
[19] Hedin E, Bäck A. Influence of different dose calculation algorithms on the estimate of NTCP for lung complications. JACMP 2013;14:127–39.
[20] Basran PS, Zavgorodni S, Berrang T, Olivotto IA, Beckham W. The impact of dose calculation algorithms on partial and whole breast radiation treatment plans. Radiat Onc 2010;5:1–9.